JOTCS A
Journal of the Turkish Chemical Society
Section: A
Chemistry
TURKISH CHEMICAL SOCIETY

Surface Physicochemical Characterization of Shepherd's Purse (*Capsella bursa-pastoris*) by Inverse Gas Chromatography

Birol Isik[1*]

[1] Yildiz Technical University, Faculty of Arts & Sciences, Department of Chemistry, Esenler, Istanbul, 34220, Turkey.

Abstract: Shepherd's purse (*Capsella bursa-pastoris*) is one of the plants widely utilized in conventional medicine and can grow in different parts of the world. The determination of the surface properties of a solid material is extremely important for the industrial use of the material and the improvement of material properties. Therefore, in this study, this plant was used as a stationary phase, and its surface characterization was performed by inverse gas chromatography technique. In this context, firstly, the plant was prepared with several pretreatments to be used in the experimental tests. The V_N values were found from the retention data obtained by passing organic solvents over the plant filled into the chromatographic column in the temperature range of 303.2–328.2 K and linear retention diagrams were drawn. The γ_S^D of the plant was calculated according to Schultz, Dorris-Gray, and Donnet-Park methods, and the suitability of the methods was compared. The ΔG_A^S values were calculated with the data obtained from the Schultz method, and the ΔH_A^S values were calculated using these data. The acidity and basicity of the plant surface were examined. According to the K_D/K_A value (0.93), it was determined that the surface of the plant was acidic.

Keywords: Adsorption, surface properties, inverse gas chromatography, shepherd's purse.

Submitted: April 6, 2023. **Accepted:** September 10, 2023.

Cite this: Isik B. Surface Physicochemical Characterization of Shepherd's Purse (*Capsella bursa-pastoris*) by Inverse Gas Chromatography. JOTCSA. 2023;10(4):1071-80.

DOI: https://doi.org/10.18596/jotcsa.1278025

***Corresponding author's E-mail:** 19birol91@gmail.com, isikb@yildiz.edu.tr

1. INTRODUCTION

A popular technique for analyzing volatiles is gas chromatography, which combines a stationary phase with known properties and an inert mobile phase. Several different types of volatile chemicals can be examined using gas chromatography (1–3). Nevertheless, this technique cannot be used to analyze large molecular weights and non-volatile components such as lignocellulosic materials (4), clays (5), liquid crystals (6), polymers (7), and composites (8). To examine such compounds, inverse gas chromatography (IGC) was improved for the task (9–11).

Unlike traditional gas chromatography, the IGC method analyzes solid materials by passing them through a chromatographic column loaded with known-property volatile solvents. The IGC approach uses retention data from experimental research to characterize the physicochemical properties of solid materials in a simple, rapid, reliable, and generally low-cost manner (12–14). The IGC approach allows for the study of both infinite dilution and restricted concentration. The parameters surface energy, acidity-basicity constants, adsorption enthalpy, entropy, and Gibbs free energy can all be obtained by doing experimental tests at infinite dilution (15,16).

The development of a solid material's qualities and optimum efficiency all depend heavily on the surface properties of the material that will be used in various industrial applications. Surface-free energy in particular is crucial for the processing and use of materials. This energy plays a crucial role in the identification, assessment, and development of material surface characteristics such as ornamentation, wetting capacity, adhesion, and coating (17,18). Measurements of liquid adsorption, flow micro-calorimetry, and contact angle can all be used to calculate the surface energy of solid materials (19,20). Researchers have recently favored the IGC methodology over these methods, however, because it is simpler to use, has higher efficiency, and produces data with higher accuracy.

This is because determining surface energy using these methods is rather limited and complex. The IGC method also determines whether the material's surface is acidic or alkaline. The material surface's acidity or basicity offers crucial preliminary data for assessing the adsorption behavior of the materials and choosing the right pollutant to maximize the efficiency of the adsorption process. Several techniques, including pH_{pzc} determination, zeta potential tests, and the Boehm titration method, can be used to determine the acidity or alkalinity of the material surface. The IGC approach, however, offers straightforward and quick findings and enables the evaluation of several surface properties in addition to acidity and alkalinity parameters (21–23).

One plant that is commonly used in conventional medicine is the shepherd's purse (*Capsella bursa-pastoris*), which is a global plant that may grow anywhere. Shepherd's purse contains a wide variety of chemicals, including flavonoids, fatty acids, organic acids, amino acids, many trace elements, vitamins, and many other compounds. This plant can be widely used for antimicrobial, anti-inflammatory, antioxidant, cardiovascular, reproductive, anticancer, sedative, and other pharmacological fields and purposes (24–27). Shepherd's purse can be utilized in many areas. Besides, as a lignocellulosic material, it has the potential to be used as an efficient sorbent for the removal of various organic contaminants and heavy metals from aqueous environments. For this purpose, it is extremely significant to investigate the surface properties of the shepherd's purse plant.

In this work, the IGC method was used to determine the surface characteristics of the shepherd's purse at infinite dilution. In this case, a chromatographic column was loaded with the powdered shepherd's purse following specific pretreatments. The plant's retention behavior was then evaluated by running various organic solvents through the column. Net retention volumes and linear retention diagrams were calculated using the retention information gleaned from the experimental research. The information obtained from these linear diagrams was used to determine the surface characteristics of the shepherd's purse.

2. EXPERIMENTAL SECTION

2.1. Materials and methods

All chemicals were illustrated in Table 1. All chemicals were acquired from Sigma Aldrich and Merck, Inc. For the chromatographic investigations, a 0.5 m stainless steel column from Alltech Associates Inc. was employed. Furthermore, from Alltech Associates Inc., silanized glass wool was utilized to fill the column tips. As the mobile phase in the IGC investigations, high-purity inert helium (He) gas was used.

Table 1. The chemicals used in this work.

Chemicals	Abbreviation	Source	CAS Registry Number	Assay
n-Hexane	Hx	Sigma Aldrich	110-54-3	≥99.7%
n-Heptane	Hp	Sigma Aldrich	142-82-5	≥99.0%
n-Octane	O	Sigma Aldrich	111-65-9	≥99.0%
n-Nonane	N	Sigma Aldrich	111-84-2	≥99.0%
n-Decane	D	Sigma Aldrich	124-18-5	≥94.0%
Tetrahydrofuran	THF	Sigma Aldrich	109-99-9	≥99.8%
Acetone	Ace	Sigma Aldrich	67-64-1	≥99.8%
Ethyl acetate	EA	Sigma Aldrich	141-78-6	≥99.8%
Chloroform	TCM	Sigma Aldrich	67-66-3	≥99.8%
Dichloromethane	DCM	Sigma Aldrich	75-09-2	≥99.8%
Diethyl ether	DEE	Sigma Aldrich	60-29-7	≥97.5%

A thermal conductivity detector-equipped Agilent Technologies 6890N gas chromatograph was used to carry out the IGC studies. The temperature of the sample injection unit and detector of the gas chromatography device used throughout the studies is 523.2 K. Several organic solvents were applied to the prepared adsorbent using a 1 mL Hamilton syringe, and their retention behavior was examined. The air peak was also obtained using a Hamilton syringe of 10 mL. Each solvent and air injection received at least four successive injections for each set of measurements to ensure the correctness of the experimental data. Retention times were calculated based on the solvents' behavior during retention on the stationary phase, and retention diagrams were drawn. The surface characteristics of the materials in the temperature range of 303.2–328.2 K were determined using these retention diagrams, and the results were evaluated. For infinite dilution, the probe (0.1 μL) was taken into the syringe and flushed into the air. Then, the air and probe retention times were calculated. For every set of measurements, each probe and air injection were received at least four consecutive times.

2.2. Preparation of the Adsorbent and Chromatographic Column

Shepherd's purse plants were bought from herbalists in Istanbul, Turkey, and then they were scrubbed clean of any dirt and dust. Then, to get rid of different pollutants and impurities, they were extensively cleaned with distilled water. At 383.2 K for 24 h, an oven was used to dry the completely washed plants (23,28). With a grinder, they were further ground to 80–100 mesh. For further research, the ground plants were dried again in an oven at 383.2 K for 48 h after being cleaned many times with distilled water.

A stainless-steel chromatographic column was cut into 0.5 m in length. It was first washed with distilled

water and then with chromic acid to remove organic and inorganic contaminants. It was then cleaned again with distilled water and passed through acetone. After this process, it was dried in an oven at 383.2 K for 24 hours. Then, sorbent was filled into the column at approximately 0.6 g. After this process, the column ends were completely plugged with silanized glass wool.

3. RESULTS AND DISCUSSION

The interaction between the shepherd's purse and organic solvents is determined by the retention time of the selected solvent. A net retention volume (V_N) is calculated by the following equation (29,30):

$$V_N = Q \times J \times (t_R - t_A) \times T/T_f \quad (1)$$

Here, t_R and t_A are the retention times of solvents and air, respectively. Q is the volumetric flow rate, J is the James-Martin constant, T is the column temperature (K), and T_f is the ambient temperature (K).

Using the retention data of the solvents on the stationary phase (shepherd's purse) in the column, V_N values were determined by equation (1) utilizing the data. Figure 1 illustrates linear retention diagrams.

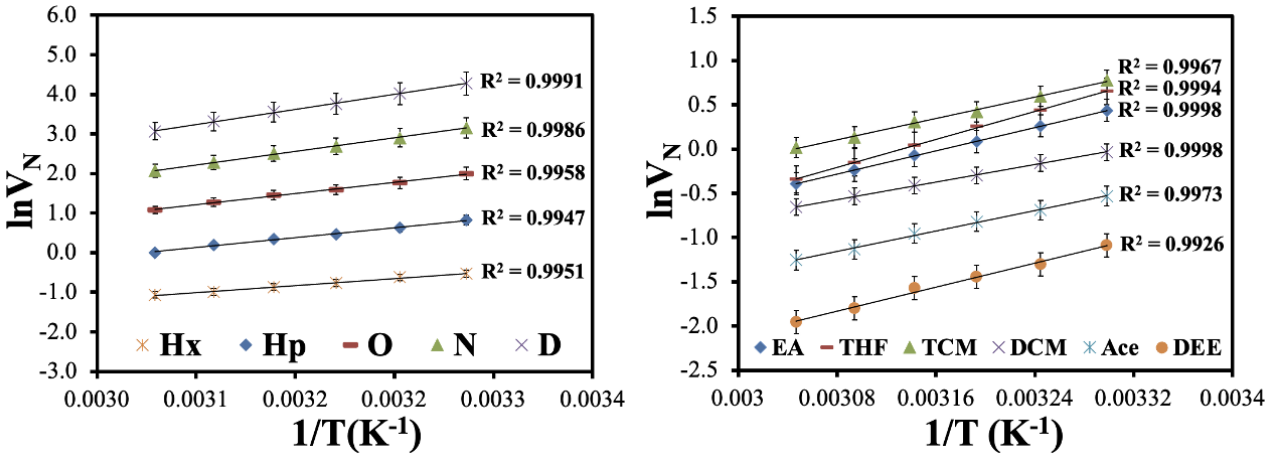

Figure 1. The linear retention diagrams of organic solvents onto shepherd's purse.

By employing the V_N values derived by equation (1) with the aid of the raw data collected from the IGC tests, it is possible to determine the Gibbs free energy of adsorption (ΔG_A^o), which is a crucial parameter for the sorption process. The ΔG_A^o values were calculated from the following equation (31–33):

$$\Delta G_A = -R \times T \times \ln(V_N) + K \quad (2)$$

The chemical composition, physical characteristics, and composition of solid materials can all affect how energetically active they are on the surface. Van der Waals interactions, which are weak, London forces, and strong interactions like acid-base and polar interactions are what cause the interactions between the solid material and organic solvent to occur (34). The dispersive surface energy (γ_S^D) is a result of the weak interaction between the solid material and solvent molecules. There are several ways to compute the γ_S^D values, including the Dorris-Gray (equation (3)) (35), Donnet-Park (36–38), and Schultz (equation (4)) (39) approaches.

$$-\Delta G_{[CH_2]} = 2 \times N_A \times a_{[CH_2]} \times \left(\gamma_S^D \times \gamma_{[CH_2]}^D\right)^{0.5} \quad (3)$$

$$-\Delta G_A = R \times T \times \ln(V_N) = 2 \times N_A \times a \times (\gamma_S^D \times \gamma_L^D)^{0.5} + K \quad (4)$$

Here, $\Delta G_{[CH_2]}$ is the Gibbs free energy of a surface including only the -CH_2 group, calculated according to equation (5). $a_{[CH_2]}$ refers to the surface area of the -CH_2 group (0.06 nm^2). "a" refers to the cross-sectional area of solvents, and γ_L^D refers to the dispersive energy of solvents. These values were taken from the literature and are presented in Table 2.

$\gamma_{[CH_2]}^D$ refers to the dispersive energy of the -CH_2 group, calculated according to the Dorris-Gray (Equation (5)) (35) and Donnet-Park (Equation (6)) (36–38) approaches.

$$\Delta G_{[CH_2]} = -R \times T \times \ln\left(\frac{V_{N,n}}{V_{N,n+1}}\right) \quad (5)$$

$$\gamma_{[CH_2]}^D = 35.6 - 0.058 \times t \quad (6)$$

$$\gamma_{[CH_2]}^D = 35.6 - 0.058 \times (t - 20) \quad (7)$$

Here, t refers to the column temperature. $V_{N,n}$ and $V_{N,n+1}$ refer to the net retention volumes of n-alkanes consisting of a n and $n+1$ carbon atoms, respectively.

Figure 2 displays $RT \ln V_N$ linear graphs versus the carbon number of n-alkanes according to equation (7), used to calculate the γ_S^D values using the Dorris-Gray equation in equation (3).

Table 2. The values of a and γ_L^D for organic solvents (29).

Probes	a (x10^{-10} m^2)	γ_L^D (mJ/m^2)
n-Hexane (Hx)	51.5	18.4
n-Heptane (Hp)	57.0	20.3
n-Octane (O)	62.8	21.3
n-Nonane (N)	69.0	22.7
n-Decane (D)	75.0	23.4
Dichloromethane (DCM)	31.5	27.6
Chloroform (TCM)	44.0	25.9
Tetrahydrofuran (THF)	45.0	22.5
Ethyl acetate (EA)	48.0	19.6
Acetone (Ace)	42.5	16.5
Diethyl ether (DEE)	47.0	15.0

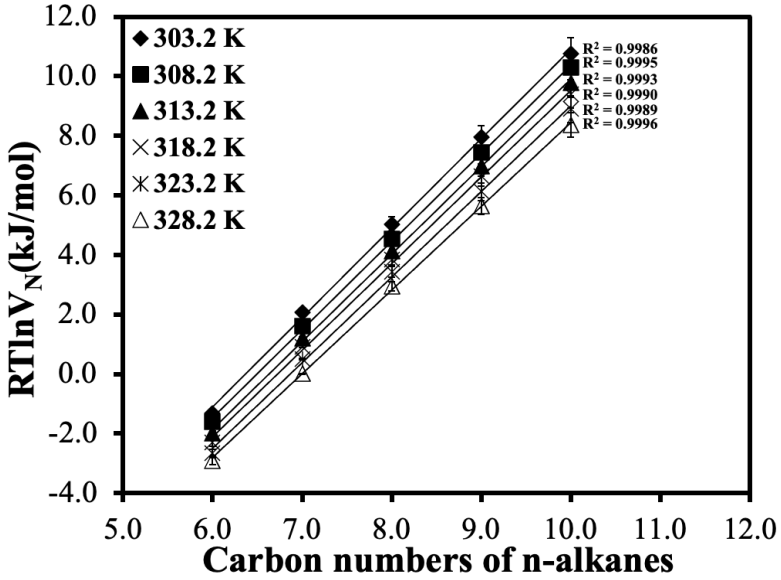

Figure 2. The linear plot of $RT \ln V_N$ versus carbon numbers of n-alkanes.

According to the Dorris-Gray and Donnet-Park methods, $\gamma_{[CH_2]}^D$ values were calculated according to equations (6) and (7), respectively, and illustrated in Table 3. By substituting the $\Delta G_{[CH_2]}$ values found from Figure 2 and the $\gamma_{[CH_2]}^D$ values calculated from equations (6) and (7) into equation (3), the γ_S^D values were found from the Dorris-Gray and Donnet-Park methods, and the results are given in Table 3.

Table 3. Dispersive surface energy (γ_S^D, mJ/m^2) values determined using the Dorris-Gray and Donnet-Park method of shepherd's purse.

	Dorris-Gray method			Donnet-Park method	
T (K)	γ_{CH_2} **(mJ/m^2)**	$-\Delta G_{ads}(CH_2)$ **(kJ/mol)**	γ_S^D **(mJ/m^2)**	γ_{CH_2} **(mJ/m^2)**	γ_S^D **(mJ/m^2)**
303.2	33.86	3.01	51.13	35.02	49.44
308.2	33.57	2.96	50.05	34.73	48.38
313.2	33.28	2.93	49.61	34.44	47.94
318.2	32.99	2.91	49.21	34.15	47.54
323.2	32.70	2.87	48.36	33.86	46.71
328.2	32.41	2.82	46.89	33.57	45.27

From Table 3, the γ_S^D values of the shepherd's purse were found in the range of 51.13–46.89 mJ/m^2 by the Dorris-Gray method and in the range of 49.44–46.89 mJ/m^2 by the Donnet-Park method. It was observed that the γ_S^D values gradually decreased with increasing temperature. In this case, it can be concluded that the decrease in surface energy with increasing temperature may facilitate coating, wetting, and bonding to different surfaces at higher temperatures. Similar results were also found in the literature. Perez-Mendoza et al. calculated the surface energies of activated carbons and found that the surface energy decreased with increasing temperature (40). Ocak et al. reported that the

surface energy of 5-((S)-3,7-dimethyloctyloxy)-2-[[[4-(dodecyloxy)phenyl]imino]-methyl]phenol liquid crystal decreases with increasing temperature (15). Erol et al. reported that the dispersive surface energy of 4-[4-((S)-citronellyloxy) benzoyloxy] benzoic acid thermotropic liquid crystal decreases with increasing temperature (30). Sreekanth et al. reported that the dispersive surface energy of thiourea and melamine polymerized graphitic carbon nitride sheets decreases with increasing temperature (41). Similarly, Papadopoulou et al. reported that the dispersive surface energy of 1-butyl-1-ethylpiperidinium bromide decreases with increasing temperature (42).

The γ_S^D values were also calculated from the linear plots (Figure 3) from the Schultz method (Equation (4)). The results were listed in Table 4. As can be seen from Table 4, the γ_S^D values were found to decrease with increasing temperature in the Schultz method. The methods used for the calculation of the γ_S^D values were found to be compatible with each other. There is a difference between the three methods because the Schultz approach determines the surface area of hydrocarbon solvent molecules based on the assumption that they are spherical, which is usually stated as a constant (43).

Table 4. Dispersive surface energy (γ_S^D, mJ/m^2) values obtained using the Schultz method of shepherd's purse.

Temperature (K)	303.2	308.2	313.2	318.2	323.2	328.2
Schultz method	49.21	47.75	46.92	46.13	44.93	43.18

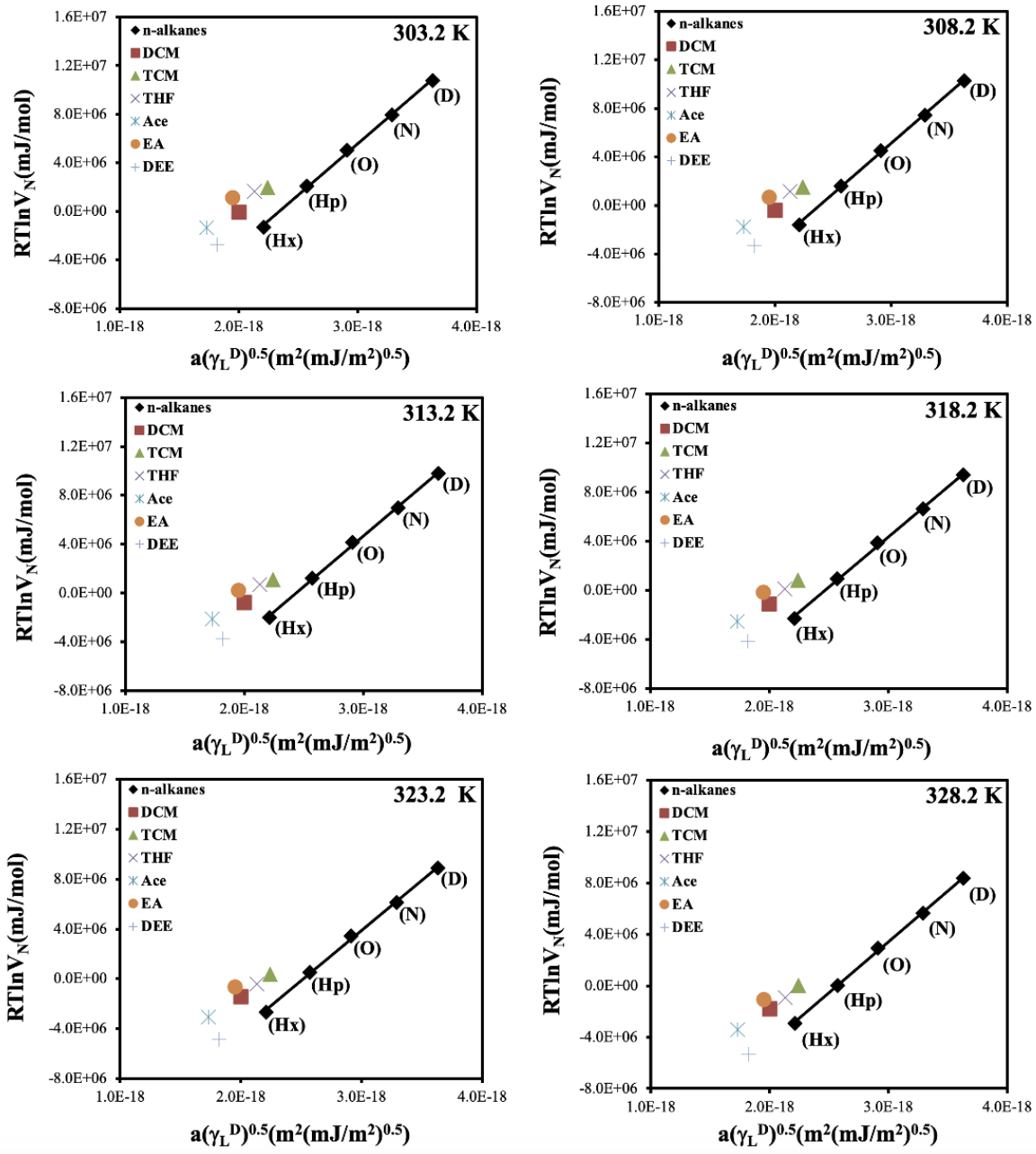

Figure 3. The linear plots drawn between $a(\gamma_L^D)^{0.5}$ and $RT \ln V_N$ values according to the Schultz method.

Figure 4 shows the comparison and temperature dependence of the three different methods applied in this study to calculate the γ_S^D values. As can be seen in Figure 4, the γ_S^D values decreased with temperature in all three approaches. From all the results, the best correlation coefficient (R^2 = 0.9822) was found in the Schultz method. The correlation coefficients of the Dorris-Gray and Donnet-Park methods are also very close to each other.

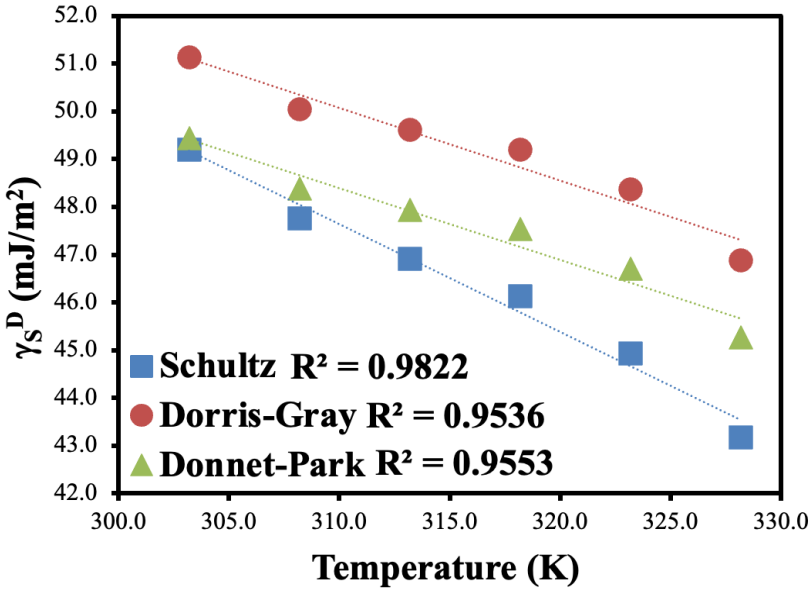

Figure 4. Variation of the γ_S^D values of shepherd's purse with temperature, as obtained by the Schultz, Dorris-Gray, and Donnet-Park approaches.

In the Schultz plots given in Figure 3, the specific Gibbs free energies (ΔG_A^S) of polar solvents were found from the distances of polar solvents to the linear line of n-alkanes and given in Table 5. From Table 5, the sorption process appears to be spontaneous. It was also found that $-\Delta G_A^S$ values decreased gradually with rising temperature.

Table 5. The $-\Delta G_A^S$ (kJ/mol) values of polar solvents onto shepherd's purse.

T (K)	EA	Ace	DCM	TCM	THF	DEE
303.2	4.41	3.83	2.80	2.82	3.44	1.66
308.2	4.31	3.70	2.81	2.75	3.27	1.37
313.2	4.22	3.67	2.81	2.69	3.19	1.30
318.2	4.06	3.52	2.74	2.69	2.88	1.15
323.2	3.95	3.31	2.74	2.61	2.73	0.80
328.2	3.52	2.94	2.40	2.29	2.21	0.30

Based on the $-\Delta G_A^S$ values presented in Table 5, the sorption enthalpy (ΔH_A^S) values were calculated using equation (8), which are then provided in Table 6 (14, 44).

$$-\frac{\Delta G_A^S}{T} = -\frac{\Delta H_A^S}{T} + \Delta S_A^S \qquad (8)$$

As seen in Table 6, the sorption process was found to be exothermic. The ΔH_A^S values for polar solvents follow the order of magnitude THF>DEE> EA>Ace>TCM>DCM. Here, THF ($DN = 84.4, AN = 2.1$) interacts better with acidic surfaces since it is a relatively basic solvent. On the contrary, since DCM ($DN = 0.0, AN = 16.4$) is a relatively acidic solvent, it interacts more with basic surfaces (45–47).

Table 6. $-\Delta H_A^S$ (kJ/mol) values of shepherd's purse for the polar solvents.

Polar Solvents	Ace	EA	THF	DCM	TCM	DEE
$-\Delta H_A^S$ **(kJ/mol)**	13.72	14.17	17.36	6.64	8.05	16.63

Polar solvents were used to determine details regarding the surface acidity or basicity of the shepherd's purse. According to the method suggested by Gutmann, the behavior of acidity or basicity can be analyzed using the following equation (48,49). The $-\Delta H_A^S$ values given in Table 6 were used to calculate the acidity or basicity character.

$$-\Delta H_A^S = K_A \times (DN) + K_D \times (AN^*) \quad (9)$$

Here, DN and AN^* refer to the donor and acceptor numbers, respectively. K_A and K_D refer to the acidity and basicity constants, respectively. If the $K_D/K_A > 1$, the sorbent surface is basic. If the $K_D/K_A < 1$, the sorbent surface is acidic.

Figure 5 shows the linear plot to calculate the acidity-basicity constants. From the slope and intercept of this linear plot, K_A and K_D values were calculated, respectively. Accordingly, the K_A value was found to be 0.1989 and the K_D value was found to be 0.1847. The K_D/K_A value calculated by using these values was found to be 0.93. According to this value, it can be said that the surface of the shepherd's purse has an acidic character. This study provides preliminary information about which type of pollutant to choose for sorption studies.

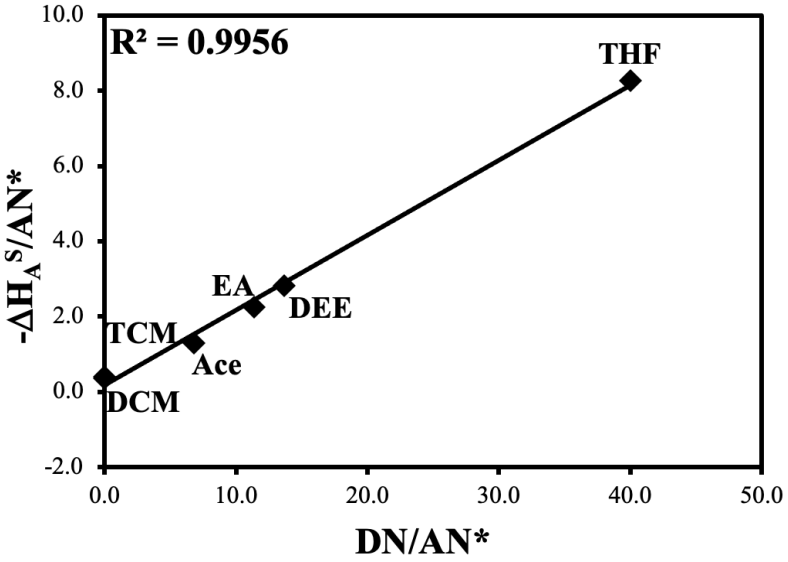

Figure 5. The plot of $-\Delta H_A^S/AN^*$ vs DN/AN^* of shepherd's purse.

4. CONCLUSION

In the current work, the stationary phase of the shepherd's purse was generated, and its surface properties were assessed using the IGC approach at infinite dilution. The retention diagrams were obtained between 303.2 and 328.2 K, and then calculations were made based on these diagrams to determine the γ_S^D, ΔH_A^S, ΔG_A^S, and K_A and K_D constants. The γ_S^D values of shepherd's purse were ranging from 51.13 to 46.89 mJ/m^2 (Dorris-Gray), 49.44 to 45.47 mJ/m^2 (Donnet-Park), and 49.21 to 43.18 mJ/m^2 (Schultz). These values were shown to be high and to decrease linearly with the increasing temperature. $K_D/K_A = 0.93$ indicate that the surface of the shepherd's purse has an acidic behavior. The process of solvents adsorbing on the shepherd's purse was found to be exothermic based on the results of enthalpy measurements. According to these results, preliminary information can be obtained about which type of pollutant should be removed from aqueous solutions when shepherd's purse is used as an adsorbent. Since the shepherd's purse surface is acidic, it can be concluded that functional groups that may show acidic properties may be present on the surface, and cationic pollutants can be removed from wastewater.

5. CONFLICT OF INTEREST

The authors declare that they have no known competing financial interests or personal relationships that could have appeared to influence the work reported in this paper.

6. REFERENCES

1. Dettmer-Wilde K, Engewald W. Practical gas chromatography [Internet]. Berlin, Heidelberg: Springer; 2014. 904 p. Available from: <URL>.

2. Smidsrød O, Guillet JE. Study of polymer-solute interactions by gas chromatography. Macromolecules [Internet]. 1969 May 1;2(3):272–7. Available from: <URL>.

3. Aresta AM, De Vietro N, Picciariello A, Rotelli MT, Altomare DF, Dezi A, et al. Volatile organic compounds determination from intestinal polyps and in exhaled breath by gas chromatography–mass spectrometry. Appl Sci [Internet]. 2023 May 15;13(10):6083. Available from: <URL>.

4. Bai W, Pakdel E, Li Q, Wang J, Tang W, Tang B, et al. Inverse gas chromatography (IGC) for studying the cellulosic materials surface characteristics: a mini review. Cellulose [Internet]. 2023 Apr 6;30(6):3379–96. Available from: <URL>.

5. Boudriche L, Calvet R, Chamayou A, Hamdi B. Influence of different wet milling on the properties of an attapulgite clay, contribution of inverse gas chromatography. Powder Technol [Internet]. 2021 Jan 22;378:29–39. Available from: <URL>.

6. Cakar F, Ocak H, Ozturk E, Mutlu-Yanic S, Kaya D, San N, et al. Investigation of thermodynamic and surface characterisation of 4-[4-(2-ethylhexyloxy)benzoyloxy]benzoic acid thermotropic liquid crystal by inverse gas chromatography. Liq Cryst [Internet]. 2014 Sep 2;41(9):1323–31. Available from: <URL>.

7. Yampolskii Y, Belov N. Investigation of polymers by inverse gas chromatography. Macromolecules [Internet]. 2015 Oct 13;48(19):6751–67. Available from: <URL>.

8. Cakar F. Synthesis and thermodynamic characterization of poly(methyl methacrylate) /multiwall carbon nanotube nanocomposite. Surf Interface Anal [Internet]. 2021 Feb 4;53(2):258–67. Available from: <URL>.

9. Adıgüzel A, Korkmaz B, Çakar F, Cankurtaran, Şenkal BF. Investigation of the surface properties of dibutyl amine modified poly(styrene) based polymer by inverse gas chromatography method. J Polym Res [Internet]. 2021 Mar 1;28(3):83. Available from: <URL>.

10. Nawawi WMFW, Lee K-Y, Kontturi E, Bismarck A, Mautner A. Surface properties of chitin-glucan nanopapers from Agaricus bisporus. Int J Biol Macromol [Internet]. 2020 Apr 1;148:677–87. Available from: <URL>.

11. Zhu Q-N, Wang Q, Hu Y-B, Abliz X. Practical Determination of the Solubility Parameters of 1-alkyl-3-methylimidazolium bromide ([CnC1im]Br, n = 5, 6, 7, 8) ionic liquids by inverse gas chromatography and the hansen solubility parameter. Molecules [Internet]. 2019 Apr 5;24(7):1346. Available from: <URL>.

12. Saada A, Papirer E, Balard H, Siffert B. Determination of the surface properties of illites and kaolinites by inverse gas chromatography. J Colloid Interface Sci [Internet]. 1995 Oct 1;175(1):212–8. Available from: <URL>.

13. Cordeiro N, Gouveia C, John MJ. Investigation of surface properties of physico-chemically modified natural fibres using inverse gas chromatography. Ind Crops Prod [Internet]. 2011 Jan 1;33(1):108–15. Available from: <URL>.

14. van Asten A, van Veenendaal N, Koster S. Surface characterization of industrial fibers with inverse gas chromatography. J Chromatogr A [Internet]. 2000 Aug 4;888(1–2):175–96. Available from: <URL>.

15. Ocak H, Mutlu-Yanic S, Cakar F, Bilgin-Eran B, Guzeller D, Karaman F, et al. A study of the thermodynamical interactions with solvents and surface characterisation of liquid crystalline 5-((S)-3,7-dimethyloctyloxy)-2-[[[4-(dodecyloxy)phenyl] imino]-methyl]phenol by inverse gas chromatography. J Mol Liq [Internet]. 2016 Nov 1;223:861–7. Available from: <URL>.

16. Uhlmann P, Schneider S. Acid–base and surface energy characterization of grafted polyethylene using inverse gas chromatography. J Chromatogr A [Internet]. 2002 Sep 6;969(1–2):73–80. Available from: <URL>.

17. Król P, Król B. Determination of free surface energy values for ceramic materials and polyurethane surface-modifying aqueous emulsions. J Eur Ceram Soc [Internet]. 2006 Jan 1;26(12): 2241–8. Available from: <URL>.

18. Ugraskan V, Isik B, Yazici O, Cakar F. Surface characterization and synthesis of boron carbide and silicon carbide. Solid State Sci [Internet]. 2021 Aug 1;118:106636. Available from: <URL>.

19. Faria PC., Órfão JJ., Pereira MF. Adsorption of anionic and cationic dyes on activated carbons with different surface chemistries. Water Res [Internet]. 2004 Apr 1;38(8):2043–52. Available from: <URL>.

20. Nassar NN, Hassan A, Pereira-Almao P. Effect of surface acidity and basicity of aluminas on asphaltene adsorption and oxidation. J Colloid Interface Sci [Internet]. 2011 Aug 1;360(1):233–8. Available from: <URL>.

21. Isik B, Cakar F, Cankurtaran O. A comparative study of surface properties of *Urtica dioica* (nettle) leaves, roots, and seeds and examination of their ability to separate xylene isomers. Phytochem Anal [Internet]. 2022 Aug 29;33(6):886–94. Available from: <URL>.

22. Gamelas JAF. The surface properties of cellulose and lignocellulosic materials assessed by inverse gas chromatography: a review. Cellulose [Internet]. 2013 Dec 1;20(6):2675–93. Available from: <URL>.

23. Isik B, Avci S, Cakar F, Cankurtaran O. Adsorptive removal of hazardous dye (crystal violet) using bay leaves (Laurus nobilis L.): surface characterization, batch adsorption studies, and statistical analysis. Environ Sci Pollut Res [Internet]. 2023 Jan 2;30(1):1333–56. Available from: <URL>.

24. Grosso C, Vinholes J, Silva LR, Pinho PG de, Gonçalves RF, Valentão P, et al. Chemical composition and biological screening of Capsella bursa-pastoris. Rev Bras Farmacogn [Internet]. 2011 Aug;21(4):635–43. Available from: <URL>.

25. Al-Snafi AE. The chemical constituents and pharmacological effects of capsella bursa-pastoris-a review. Int J Pharmacol Toxicol [Internet]. 2015;5(2):76–81. Available from: <URL>.

26. Al-Douri NA, Al-Essa LY. A survey of plants used in Iraqi traditional medicine. Jordan J Pharm Sci [Internet]. 2010 Jul 12;3(2):100–18. Available from: <URL>.

27. Alizadeh H, Club YR, Branch A, Jafari B, Babae T. The Study of Antibacterial Effect of Capsella Bursa-

Pastoris on Some of Gram Positive and Gram Negative Bacteria. J Basic Appl Sci Res [Internet]. 2012;2(7):6940–5. Available from: <URL>.

28. Ali NS, Jabbar NM, Alardhi SM, Majdi HS, Albayati TM. Adsorption of methyl violet dye onto a prepared bio-adsorbent from date seeds: isotherm, kinetics, and thermodynamic studies. Heliyon [Internet]. 2022 Aug 1;8(8):e10276. Available from: <URL>.

29. Işık B, Çakar F, Cankurtaran H, Cankurtaran Ö. Evaluation of the surface properties of 4-(Decyloxy) benzoic acid liquid crystal and its use in structural isomer separation. Turkish J Chem [Internet]. 2021 Jun 30;45(3):845–57. Available from: <URL>.

30. Erol I, Cakar F, Ocak H, Cankurtaran H, Cankurtaran Ö, Bilgin-Eran B, et al. Thermodynamic and surface characterisation of 4-[4-((S)-citronellyloxy)benzoyloxy]benzoic acid thermotropic liquid crystal. Liq Cryst [Internet]. 2016 Jan 2;43(1):142–51. Available from: <URL>.

31. Mukhopadhyay P, Schreiber HP. Aspects of acid-base interactions and use of inverse gas chromatography. Colloids Surfaces A Physicochem Eng Asp [Internet]. 1995 Jul 25;100:47–71. Available from: <URL>.

32. Isik B, Cakar F, Cankurtaran O, Cankurtaran H. Liquid crystal entrapped porous films for ammonia sensing and determination of surface properties of liquid crystal molecule. ChemistrySelect [Internet]. 2021 Jul 13;6(26):6740–7. Available from: <URL>.

33. Ugraskan V, Isik B, Yazici O, Cakar F. Comparative physicochemical characterization of ULTEM/SWCNT nanocomposites: Surface, thermal and electrical conductivity analyses. J Polym Res [Internet]. 2022 Jul 2;29(7):254. Available from: <URL>.

34. Ugraskan V, Isik B, Yazici O, Cakar F. Removal of Safranine T by a highly efficient adsorbent (Cotinus Coggygria leaves): Isotherms, kinetics, thermodynamics, and surface properties. Surfaces and Interfaces [Internet]. 2022 Feb 1;28:101615. Available from: <URL>.

35. Dorris GM, Gray DG. Adsorption of n-alkanes at zero surface coverage on cellulose paper and wood fibers. J Colloid Interface Sci [Internet]. 1980 Oct 1;77(2):353–62. Available from: <URL>.

36. Donnet J-B, Park S-J. Surface characteristics of pitch-based carbon fibers by inverse gas chromatography method. Carbon N Y [Internet]. 1991 Jan 1;29(7):955–61. Available from: <URL>.

37. Donnet JB, Park SJ, Balard H. Evaluation of specific interactions of solid surfaces by inverse gas chromatography. Chromatographia [Internet]. 1991 May;31(9–10):434–40. Available from: <URL>.

38. Donnet JB, Park SJ, Brendle M. The effect of microwave plasma treatment on the surface energy of graphite as measured by inverse gas chromatography. Carbon N Y [Internet]. 1992 Jan 1;30(2):263–8. Available from: <URL>.

39. Schultz J, Lavielle L, Martin C. The Role of the interface in carbon fibre-epoxy composites. J Adhes [Internet]. 1987 Sep 3;23(1):45–60. Available from: <URL>.

40. Pérez-Mendoza M, Almazán-Almazán MC, Méndez-Liñán L, Domingo-García M, López-Garzón FJ. Evaluation of the dispersive component of the surface energy of active carbons as determined by inverse gas chromatography at zero surface coverage. J Chromatogr A [Internet]. 2008 Dec 19;1214(1–2):121–7. Available from: <URL>.

41. Sreekanth TVM, Basivi PK, Nagajyothi PC, Dillip GR, Shim J, Ko TJ, et al. Determination of surface properties and Gutmann's Lewis acidity–basicity parameters of thiourea and melamine polymerized graphitic carbon nitride sheets by inverse gas chromatography. J Chromatogr A [Internet]. 2018 Dec 14;1580:134–41. Available from: <URL>.

42. Papadopoulou SK, Papaiconomou N, Baup S, Iojoiu C, Svecova L, Thivel P-X. Surface characterization of 1-butyl-1-ethylpiperidinium bromide by inverse gas chromatography. J Mol Liq [Internet]. 2019 Aug 1;287:110945. Available from: <URL>.

43. Wang Q, Wang Q. Evaluation of the surface properties of poly(ionic liquid) materials by inverse gas chromatography. Eur Polym J [Internet]. 2020 Jan 15;123:109451. Available from: <URL>.

44. Isik B, Cakar F, Cankurtaran O. The study on cholesteryl chloroformate liquid crystal for separation of isomers and determination of its surface properties. Sep Sci Technol [Internet]. 2022 Nov 22;57(17):2843–51. Available from: <URL>.

45. Santos JMRCA, Guthrie JT. Study of a core-shell type impact modifier by inverse gas chromatography. J Chromatogr A [Internet]. 2005 Apr 8;1070(1–2):147–54. Available from: <URL>.

46. Santos JMRCA, Guthrie JT. Analysis of interactions in multicomponent polymeric systems: The key-role of inverse gas chromatography. Mater Sci Eng R Reports [Internet]. 2005 Oct 31;50(3):79–107. Available from: <URL>.

47. Santos JMRCA, Fagelman K, Guthrie J. Characterisation of the surface Lewis acid–base properties of poly(butylene terephthalate) by inverse gas chromatography. J Chromatogr A [Internet]. 2002 Sep 6;969(1–2):111–8. Available from: <URL>.

48. Gutmann V. The donor-acceptor approach to molecular interactions [Internet]. Springer New York, NY; 1978. 279 p. Available from: <URL>.

49. Bauer F, Meyer R, Czihal S, Bertmer M, Decker U, Naumov S, et al. Functionalization of porous siliceous materials, Part 2: Surface characterization by inverse gas chromatography. J Chromatogr A [Internet]. 2019 Oct 11;1603:297–310. Available from: <URL>.